Single Amino Acid Substitution in the Fc Region of Chimeric TNT-3 Antibody Accelerates Clearance and Improves Immunoscintigraphy of Solid Tumors

Jason L. Hornick, Jahangir Sharifi, Leslie A. Khawli, Peisheng Hu, Wei Guo Bai, Mian M. Alauddin, Myra M. Mizokami, and Alan L. Epstein

Departments of Pathology and Radiology, University of Southern California School of Medicine, Los Angeles, California

Recent studies in antibody catabolism have identified residues at the C_H2–C_H3 interface of the IgG heavy chain critical for serum persistence of immunoglobulins. Amino acid substitutions in the Fc region of murine IgG_1 were shown to drastically accelerate antibody clearance in mice. Our laboratory has previously described a human–mouse chimeric TNT-3 (chTNT-3) monoclonal antibody directed against a universal nuclear antigen that has potential for the radioimmunotherapy of many solid tumors. In the current study, we engineered a chTNT-3 mutant containing a single amino acid substitution, to determine whether a more rapid clearance profile would make the antibody suitable for diagnostic imaging. **Methods:** A single amino acid substitution in the C_H2 domain of the human γ1 constant region was made by polymerase chain reaction mutagenesis. High-level expression was achieved using the Glutamine Synthetase Gene Amplification System, and the chTNT-3 mutant was purified by protein A affinity and ion-exchange chromatography. A radioimmunoassay was performed to examine antigen binding, and in vivo studies were undertaken to evaluate clearance and tumor targeting in human tumor xenograft models. **Results:** The chTNT-3 mutant retained the high affinity of chTNT-3, with a binding constant of 1.5×10^{-9} mol/L. The mutant was eliminated rapidly from BALB/c mice, with a β-phase half-life of 33.8 h, compared to 134.2 h for chTNT-3. Moreover, biodistribution studies in human colon tumor-bearing nude mice reflected this accelerated clearance. Tumor levels of the mutant were, respectively, 65%, 39%, and 36% of the tumor levels achieved with the parental chTNT-3 6, 12, and 24 h postinjection. The rapid clearance of the chTNT-3 mutant from the blood resulted in higher tumor-to-normal organ ratios for many normal tissues. Imaging of tumor-bearing mice with ^{99m}Tc-labeled chTNT-3 mutant demonstrated early visualization of tumors in 3 different solid tumor xenograft models. **Conclusion:** The accelerated clearance produced by a single amino acid substitution in the Fc region of chTNT-3 leads to improved imaging in tumor-bearing mice. These studies suggest that a rapidly clearing antibody generated by this approach may be useful for the immunoscintigraphy of human tumors.

Key Words: chimeric monoclonal antibody; pharmacokinetics; immunoscintigraphy; tumor targeting; FcRn

J Nucl Med 2000; 41:355–362

Received Oct. 25, 1998; revision accepted Jun. 21, 1999.

For correspondence or reprints contact: Alan L. Epstein, MD, PhD, University of Southern California School of Medicine, Department of Pathology, 2011 Zonal Ave., HMR 210, Los Angeles, CA 90033.

The clinical potential of monoclonal antibodies (MAbs) for the diagnostic imaging of human malignancies has begun to be realized during the past decade, as evidenced by the approval of 4 antibodies and derived fragments for the immunoscintigraphy of tumors (*1–4*). Although the successful introduction of these products into the clinical armamentarium of imaging agents underscores the value of antibodies for cancer detection, the problems posed by the pharmacokinetic behavior of antibodies and fragments in patients remain. Because intact antibodies clear slowly, they are less-than-ideal imaging reagents; circulating radiolabeled antibody obscures tumor visualization until sufficient antibody has cleared. Typically, clinicians must wait 2–5 d after administration of radiolabeled intact antibodies before useful images can be obtained (*1,4*). On the other hand, antibody fragments such as Fab′ clear extremely rapidly, allowing for early discrimination of tumors (*2,3*). The predominant renal clearance of monovalent fragments, however, results in the accumulation of signal in the kidneys and bladder (*5,6*), which can impede the identification of tumors in the abdomen and pelvis. Moreover, the substantially reduced tumor accretion of antibody fragments compared to intact antibodies (*5,7,8*) secondary to their rapid clearance can decrease their sensitivity for detecting tumor sites. An understanding of the mechanism responsible for antibody clearance would allow antibodies to be developed with improved pharmacokinetic behavior.

Recent studies have identified critical amino acid residues within murine IgG that maintain serum persistence through interactions with the FcRn receptor (*9*). These experiments have demonstrated that single amino acid substitutions within the C_H2 or C_H3 domain of murine IgG_1 Fc fragments result in rapid clearance of the mutated fragments from mice, presumably as a result of decreased binding to FcRn (*10,11*). This breakthrough in understanding of the mechanism underlying immunoglobulin catabolism may have profound implications for antibody imaging and therapy in patients, because antibody engineering may now produce

tailor-made antibodies selected for their pharmacokinetic behavior (*12*).

Our laboratory has previously described a human–mouse chTNT-3 MAb directed against a universal nuclear antigen with potential for radioimmunotherapy of the majority of solid tumors (*13*). In the current study, we sought to engineer a chTNT-3 mutant containing a single amino acid substitution in a conserved residue that has been shown to be critical for maintaining serum persistence of murine IgG_1 and to evaluate its potential utility in cancer diagnosis by pharmacokinetic, biodistribution, and immunoscintigraphic studies in mouse models.

MATERIALS AND METHODS

Reagents

The plasmids pEE6hCMV-B and pEE12 were purchased with the Glutamine Synthetase Gene Amplification System from Lonza Biologics (Slough, UK). Restriction endonucleases, T4 DNA ligase, and other molecular biology reagents were purchased from New England Biolabs (Beverly, MA) or Boehringer Mannheim (Indianapolis, IN). Dialyzed fetal bovine serum, single-stranded DNA from calf thymus, chloramine T, and 2,2′-azino-bis(3-ethylbenzthiazoline-6-sulfonic acid) diammonium salt (ABTS) were purchased from Sigma Chemical Co. (St. Louis, MO). ^{125}I was obtained as sodium iodide in 0.1 *N* sodium hydroxide from DuPont/New England Nuclear (North Billerica, MA). ^{99m}Tc-sodium pertechnetate was obtained from Syncor International Corp. (Van Nuys, CA). BALB/c and athymic nude mice were purchased from Harlan Sprague-Dawley (Indianapolis, IN).

Antibody and Cell Lines

The chimeric MAb TNT-3 (chTNT-3, $IgG_1\kappa$) was produced as described previously (*13*). The NS0 murine myeloma cell line was obtained from Lonza Biologics. The Raji cell line, derived from an African Burkitt's lymphoma (*14,15*), the LS174T human colon adenocarcinoma cell line (*16*), the A427 human lung adenocarcinoma cell line (*17*), and the LNCaP human prostatic adenocarcinoma cell line (*18*) were obtained from the American Type Culture Collection (Manassas, VA).

Construction of Expression Vectors

The mutant chimeric heavy chain was produced by polymerase chain reaction (PCR) mutagenesis, to substitute alanine for isoleucine at site 253. The expression vector for the chTNT-3 heavy chain, pEE12/chTNT-3 HC (*13*), was used as the template. Primary PCR was performed to yield overlapping heavy-chain fragments. For the upstream fragment, the 5′ TNT-3 VH leader sequence primer 5′-AGCTCTAGAGCCGCCACCATGGGATGGAGCGG-GATCTTT-3′ and the 3′ mutating primer 5′-AGGGGTCCGGGAG-GCCATGAGGGT-3′ were used, and for the downstream fragment, the 5′ mutating primer 5′-ACCCTCATGGCCTCCCGGAC-CCCT-3′ and the 3′ human γ1 primer 5′-GAAGTCGAATTCT-CATTTACCCGGGGACAGGGAGAGGCT-3′ were used. Mutated bases are indicated by underlining. A secondary PCR assembly was performed using the overlapping primary PCR fragments and the outer primers listed previously. The final assembled PCR fragment was then inserted into the XbaI and EcoRI sites of pEE12, resulting in the expression vector 12/chTNT-3 HC-253, encoding the chimeric TNT-3 heavy chain with a single amino acid substitution in the C_H2 domain of human γ1. The expression vector for the chimeric TNT-3 light chain, pEE6/chTNT-3 LC, was constructed as described previously (*13*).

Expression and Purification of the chTNT-3 Mutant

The chTNT-3 mutant was expressed from NS0 murine myeloma cells according to the manufacturer's protocol (Lonza Biologics). The highest-producing clone was incubated in a 3-L bioreactor, and the chTNT-3 mutant was purified stepwise from cell culture medium by protein A affinity chromatography and ion-exchange chromatography, as described previously (*19*). The purity of the mutant MAb was examined both by sodium dodecyl sulfate-polyacrylamide gel electrophoresis (SDS-PAGE) (*20*) and by high-performance liquid chromatography (HPLC), using a Beckman HPLC Gold System (Beckman Instruments, Inc., Fullerton, CA). Size-exclusion chromatography was performed on a G4000SW column (TosoHaas; Montgomeryville, PA) with 0.1 mol/L PBS, pH 7.2 as the solvent system, eluting at a flow rate of 1 mL/min. The ultraviolet absorbance of the HPLC eluate was detected at 280 nm.

Enzyme-Linked Immunosorbent Assay

Mutant MAb-containing supernatants were initially identified by indirect enzyme-linked immunosorbent assay (ELISA) using microtiter plates coated with single-stranded DNA from calf thymus, as described previously (*13*). For production rate assays, 10^6 cells were plated in 1 mL of medium and allowed to incubate for 24 h. Supernatants were serially diluted and applied to wells of microtiter plates coated with goat antihuman IgG (H + L) (CalTag, South San Francisco, CA). Dilutions of a control chimeric MAb were used to generate a standard curve, using a four-parameter fit by an automated ELISA reader (Bio-Tek Instruments, Inc., Winooski, VT), from which concentrations of unknowns were interpolated. Rates of production expressed as μg/mL/10^6 cells/24 h were compared to identify the highest-producing clones.

Radiolabeling of chTNT-3 and the chTNT-3 Mutant

^{125}I-labeled MAbs were prepared using a modified chloramine T method, as described previously (*19*). Radioiodinated antibodies were analyzed using an analytical instant thin-layer chromatography system, and in vitro serum stability was evaluated as described previously (*13*). Briefly, ^{125}I-labeled MAbs were incubated for 7 d in mouse serum at 37°C. After trichloroacetic acid precipitation and centrifugation, protein-bound radioactivity was measured in a γ counter.

^{99m}Tc-labeled MAbs were prepared using a modified direct labeling method essentially as previously described (*21*). The MAbs were diluted to 0.4 mg/mL in a volume of 500 μL using 0.1 mol/L sodium borate buffer, pH 9.3, deoxygenated by bubbling N_2 gas through the solution, and sealed under nitrogen. ^{99m}Tc-sodium pertechnetate (111 MBq in 300 μL) was injected into the MAb solution. Subsequently, 40 μL stannous chloride/glucoheptanoic acid solution (containing 10 mg glucoheptanoic acid and 1 mg stannous chloride in 1 mL deoxygenated water) were added to the preceding solution. The reaction mixture was incubated for 2 h at 37°C before it was purified using a PD-10 column (Pharmacia Biotech, Piscataway, NJ), with a yield of 60%–67% radiolabeled product. The MAbs were stored at 4°C and administered to mice within 1–2 h of labeling.

The in vitro stability of ^{99m}Tc-labeled MAbs was evaluated using diethylenetriaminopentaacetic acid (DTPA) as a challenging agent. A 0.2-mL aliquot of ^{99m}Tc-labeled MAb solution was placed in a vial with a 500 molar excess of DTPA and incubated at 37°C for 24 h. The reaction mixture was then analyzed by paper chromatog-

raphy using Whatman filter paper. Strips (1 × 6 cm) were spotted with 1 μL of sample and eluted with 0.9% NaCl to approximately 5 cm, dried, and cut in half. The protein-bound and non–protein-bound radioactivity was measured in a γ counter.

Determination of Avidity

The avidity constant of the chTNT-3 mutant was determined by a fixed-cell RIA, using the method of Frankel and Gerhard (*22*), as described previously (*19*). Briefly, Raji lymphoma cells fixed in 2% paraformaldehyde (*23*) were incubated with increasing amounts of ^{125}I-labeled MAb for 1 h with constant mixing. The cells were then washed and the radioactivity measured in a γ counter. The amount of MAb bound was determined by the remaining cell-bound radioactivity (cpm) in each tube and the specific activity (cpm/ng) of the radiolabeled antibody. Scatchard analysis was performed to obtain the slope. The equilibrium or avidity constant K_a was calculated by the equation $K = -(\text{slope}/n)$, where n is the valence of the antibody (2 for IgG).

Pharmacokinetic and Biodistribution Studies

It has previously been demonstrated that half-life values of IgG clearance from mice determined by whole-body dosimetry are statistically indistinguishable from those calculated by blood sampling (*24*). Whole-body dosimetry was therefore performed for this pharmacokinetic study. Six-week-old BALB/c mice were used to determine the clearance of the chTNT-3 mutant. A group of mice (n = 5), previously fed potassium iodine in drinking water for 1 wk to block thyroid uptake of radioiodine, were injected intravenously with ^{125}I-labeled MAb (1.1–1.5 MBq/mouse). The whole-body activity immediately postinjection and at selected times thereafter was measured with a CRC-7 microdosimeter (Capintec, Inc., Pittsburgh, PA). The data were analyzed and half-life was determined as described previously (*25*).

To determine the tissue biodistribution of the chTNT-3 mutant, 6-wk-old female athymic nude mice were injected subcutaneously in the left thigh with a 0.2 mL inoculum containing 2×10^7 LS174T colon adenocarcinoma cells. The tumors were grown for 10–14 d until they reached approximately 1 cm in diameter. Within each group (n = 5), individual mice were injected intravenously with a 0.1 mL inoculum containing 3.7 MBq/10 μg ^{125}I-labeled chTNT-3 or the chTNT-3 mutant. Animals were killed by sodium pentobarbital overdose 6, 12, and 24 h postinjection, and tissues were removed, weighed, and measured in a γ counter. For each mouse, data were expressed as median percentage of injected dose per gram (%ID/g) and median tumor-to-organ ratio (cpm per gram tumor/cpm per gram organ). Significance levels were determined using the Wilcoxon's rank-sum test.

Imaging Studies

Six-week-old female athymic nude mice were injected subcutaneously in the left thigh with A427 human lung adenocarcinoma cells or LS174T human colon adenocarcinoma cells, and 6-wk-old male nude mice were injected similarly with LNCaP human prostatic adenocarcinoma cells. The tumors were grown for 10–14 d (A427 and LS174T) or up to 8 wk (LNCaP) until they reached approximately 1 cm in diameter. Groups of mice (n = 3–5) were injected intravenously with a 0.1 mL inoculum containing 7.4 MBq/10 μg ^{99m}Tc-labeled chTNT-3 or the chTNT-3 mutant. At 6, 12, and 24 h postinjection, the mice were anesthetized with a subcutaneous injection of 0.8 mg sodium pentobarbital. The immobilized mice were then imaged in a prone position using a Spectrum 91 γ camera equipped with a pinhole collimator (Raytheon Medical Systems, Melrose Park, IL) set to record 10,000 counts using the Nuclear MAX Plus image analysis program (MEDX Inc., Wood Dale, IL). To determine which normal tissues contained residual signal, biodistribution of ^{99m}Tc-labeled chTNT-3 mutant was calculated for the group of mice bearing LS174T human colon adenocarcinoma tumors at the completion of the imaging study, as described earlier.

RESULTS

Construction, Expression, and Purification of the chTNT-3 Mutant

PCR mutagenesis was used to introduce mutations within the C_H2 domain of the human γ1 constant region, resulting in the substitution of isoleucine with alanine at residue 253. The assembled mutagenized PCR product was cloned into the pEE12 vector, resulting in the expression vector 12/chTNT-3 HC-253. This expression vector was cotransfected with the expression vector for the chimeric TNT-3 light chain, pEE6/chTNT-3 LC, into NS0 murine myeloma cells, and the chimeric MAb was expressed using the Glutamine Synthetase Gene Amplification System. The highest-producing subclone was scaled up to a 3-L bioreactor, and the chTNT-3 mutant was purified from spent cell culture medium, with a yield of greater than 30 μg/mL. Reducing SDS–PAGE revealed 2 discrete bands of approximately 55 and 25 kDa, corresponding to the predicted molecular weights of chimeric immunoglobulin heavy and light chains (data not shown). In addition, the purity and proper assembly of the mutant were confirmed by HPLC, which demonstrated a single sharp peak with a retention time of approximately 625 s.

Radiolabeling Efficiency and Stability

ITLC analysis of ^{125}I-labeled chTNT-3 and the chTNT-3 mutant revealed an R_f value of 0 (protein bound) and a radiochemical purity of greater than 99%. Both MAbs were examined for deiodination in mouse serum over a 7-d incubation period at 37°C. Approximately 95% of the activity was trichloroacetic-acid precipitable for both chTNT-3 and the chTNT-3 mutant; virtually no release of free radioiodine was detected over this time period. These observations provide evidence for similarities in radiolabeling efficiency and serum stability of chTNT-3 and the chTNT-3 mutant.

Paper chromatography of ^{99m}Tc-labeled chTNT-3 and the chTNT-3 mutant revealed 98% of the radioactivity remaining at the origin, indicating that ^{99m}Tc was conjugated to the MAbs. Stability of the radiolabeled MAbs was evaluated by incubating aliquots with excess DTPA at 37°C for 24 h. At each time point during incubation, no evidence of transchelation of ^{99m}Tc from the MAbs to DTPA was seen, indicating a high degree of stability of the radiolabel.

Avidity Determination

A binding study was conducted in which ^{125}I-labeled chTNT-3 mutant was incubated with fixed Raji cells and the bound radioactivity was used to calculate the avidity con-

stant K_a by Scatchard analysis. As expected, the single amino acid substitution in the Fc region had no effect on binding. The chTNT-3 mutant was found to have an avidity constant of 1.5×10^{-9} mol/L, compared with 1.4×10^{-9} mol/L for chTNT-3 (*13*). This study demonstrates that the mutant retains the binding properties of chTNT-3.

Pharmacokinetic Studies

Clearance studies in BALB/c mice were performed to establish differences in pharmacokinetics between the parental chTNT-3 and the chTNT-3 mutant. Since whole-body dosimetry was used, only the terminal β phase of clearance could be calculated. Data from 19 h onward were used to calculate clearance to avoid contributions of the α phase. It has previously been shown that chTNT-3 clears slowly from BALB/c mice with a whole-body half-life of 134.2 ± 4.0 h, typical of a chimeric MAb containing human IgG_1 constant regions (*13*). As depicted in Figure 1, the chTNT-3 mutant was eliminated significantly more rapidly with a β-phase half-life of 33.8 ± 1.0 h ($P \leq 0.01$).

Tumor-Targeting Studies

The tumor and normal tissue biodistribution of ^{125}I-labeled chTNT-3 and the chTNT-3 mutant was examined in LS174T human colon adenocarcinoma tumor-bearing nude mice 6, 12, and 24 h postinjection. Despite its rapid elimination, the mutant retains the ability to localize to tumor xenografts. By 6 h postinjection, tumor uptake of the chTNT-3 mutant was 5.34 %ID/g (Table 1), which represents approximately 65% of the tumor accretion of the parental chimeric MAb (8.18 %ID/g). By 12 h, tumor uptake of the mutant was 39% of the uptake of chTNT-3 (3.78 and 9.60 %ID/g, respectively; Table 2). The accelerated clearance of the chTNT-3 mutant produced higher tumor-to-normal organ ratios for many normal tissues, illustrating the specificity of tumor targeting with the mutant and its rapid elimination from the blood and organs. By 24 h, tumor uptake of the mutant was 2.25 %ID/g, whereas tumor accretion of chTNT-3 was 6.24 %ID/g (Table 3). These studies establish that the whole-body half-life of an IgG is a critical factor in determining tissue biodistribution and the magnitude of tumor uptake.

Immunoscintigraphy was also performed to examine the differences between tumor targeting with chTNT-3 and the mutant derivative. Groups of LNCaP human prostate tumor-

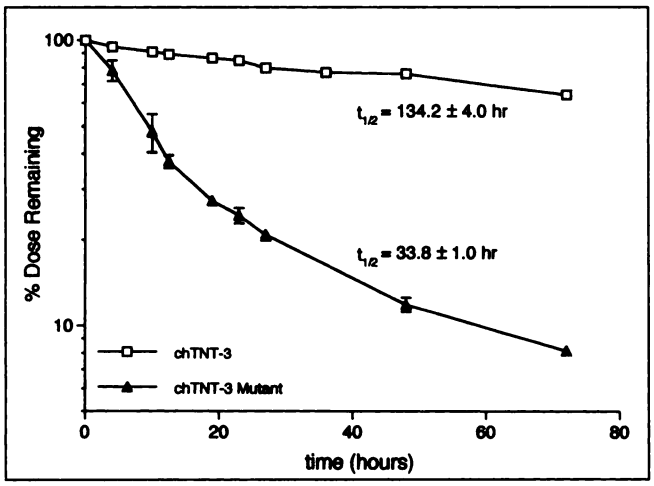

FIGURE 1. Semilog plot of whole-body pharmacokinetic clearance of ^{125}I-labeled chimeric antibodies in non–tumor-bearing BALB/c mice. Activity at injection and at selected times thereafter was measured with microdosimeter. Error bars represent 1 SD.

TABLE 1
6-Hour Biodistribution of ^{125}I-Labeled Chimeric Antibodies in LS174T Human Colon Adenocarcinoma Tumor-Bearing Nude Mice

	%ID/g			Tumor-to-organ ratio		
Organ	chTNT-3	chTNT-3 mutant	*P**	chTNT-3	chTNT-3 mutant	*P**
Blood	11.86	4.72	≤0.005	0.78	1.15	NS
Skin	2.76	1.69	≤0.01	2.79	3.18	NS
Muscle	0.32	0.31	NS	25.02	17.13	NS
Bone	1.37	0.68	NS	6.18	8.10	NS
Heart	3.49	1.18	≤0.005	2.41	4.56	NS
Lung	4.12	1.37	≤0.01	2.35	2.96	NS
Liver	1.93	1.75	NS	4.23	2.76	NS
Spleen	3.61	2.00	≤0.025	2.24	2.33	NS
Pancreas	0.89	0.63	≤0.025	8.93	7.44	NS
Stomach	1.18	4.68	≤0.005	6.74	1.15	≤0.005
Intestine	0.92	1.10	NS	8.34	4.07	≤0.05
Kidney	3.43	1.94	≤0.005	2.57	2.81	NS
Tumor	8.18	5.34	≤0.005			

*P values determined by Wilcoxon rank-sum test.
NS = not significant.

TABLE 2
12-Hour Biodistribution of ^{125}I-Labeled Chimeric Antibodies in LS174T Human Colon Adenocarcinoma Tumor-Bearing Nude Mice

	%ID/g			Tumor-to-organ ratio		
Organ	chTNT-3	chTNT-3 mutant	*P**	chTNT-3	chTNT-3 mutant	*P**
Blood	6.98	1.25	≤0.005	1.44	3.02	≤0.005
Skin	3.46	1.11	≤0.005	2.74	3.67	≤0.025
Muscle	0.67	0.18	≤0.005	13.01	21.30	≤0.005
Bone	1.59	0.48	≤0.005	6.02	7.55	≤0.05
Heart	2.63	0.64	≤0.005	3.65	5.98	≤0.01
Lung	3.96	0.55	≤0.005	2.59	6.81	≤0.005
Liver	3.37	1.41	≤0.005	2.85	2.66	NS
Spleen	3.25	2.16	≤0.005	2.97	2.01	NS
Pancreas	1.08	0.33	≤0.005	8.88	13.20	≤0.005
Stomach	2.17	1.30	≤0.005	3.89	3.33	NS
Intestine	3.21	0.84	≤0.005	3.00	4.26	NS
Kidney	2.62	0.71	≤0.005	3.91	5.34	≤0.01
Tumor	9.60	3.78	≤0.005			

*P values determined by Wilcoxon rank-sum test.
NS = not significant.

TABLE 3
24-Hour Biodistribution of ^{125}I-Labeled Chimeric Antibodies in LS174T Human Colon Adenocarcinoma Tumor-Bearing Nude Mice

	%ID/g			Tumor-to-organ ratio		
Organ	chTNT-3	chTNT-3 mutant	*P**	chTNT-3	chTNT-3 mutant	*P**
Blood	4.35	0.94	≤0.005	1.66	2.38	≤0.05
Skin	1.83	0.93	≤0.005	3.59	2.58	≤0.01
Muscle	0.35	0.15	≤0.01	17.08	15.06	NS
Bone	0.92	0.54	≤0.005	6.79	4.37	NS
Heart	1.65	0.51	≤0.005	3.29	5.89	≤0.05
Lung	2.15	0.58	≤0.005	3.09	3.55	NS
Liver	2.28	0.76	≤0.005	2.78	4.00	NS
Spleen	3.21	1.49	≤0.005	2.16	1.51	NS
Pancreas	0.45	0.29	≤0.005	16.45	9.59	≤0.05
Stomach	1.38	0.63	≤0.025	5.45	3.52	NS
Intestine	1.15	0.60	NS	6.49	3.73	NS
Kidney	1.32	0.43	≤0.005	4.10	5.22	NS
Tumor	6.24	2.25	≤0.005			

**P* values determined by Wilcoxon rank-sum test.
NS = not significant.

bearing nude mice were injected with either ^{99m}Tc-labeled chTNT-3 or the chTNT-3 mutant and imaged 6, 12, and 24 h postinjection. Images obtained from representative mice are presented in Figure 2. Visualization of the tumor uptake of chTNT-3 is obscured by the considerable signal in the blood pool and normal organs up to and including 24 h postinjection (Fig. 2A). In contrast, tumor uptake of the chTNT-3 mutant is distinct as early as 12 h postinjection, with little evidence of signal in the normal tissues of the mice after 24 h (Fig. 2B).

Immunoscintigraphy with the chTNT-3 mutant was extended to 2 additional tumor xenograft models. Figure 2C depicts imaging with ^{99m}Tc-labeled chTNT-3 mutant in LS174T human colon tumor-bearing mice, whereas Figure 2D demonstrates imaging in A427 human lung tumor-bearing mice. These studies confirm that similar results can be obtained in a variety of solid-tumor xenograft models, which can be attributed to the specificity of TNT-3 for DNA, a universal nuclear antigen accessible in the degenerating and necrotic cells within most solid tumors (*13*). Again, early visualization of the transplanted tumors and rapid clearance from the blood pool were observed. Tissue biodistribution analysis demonstrated that, aside from the tumor, the signal remaining in the bodies of mice 24 h after administration of ^{99m}Tc-labeled chTNT-3 mutant corresponds to kidney uptake (Table 4), which has previously been observed when ^{99m}Tc is used for antibody tumor targeting (*26*).

DISCUSSION

In this study, a chimeric TNT-3 antibody mutant was produced by PCR mutagenesis that contains a single amino acid substitution in the C_H2 domain of the human γ1 constant region (Ile253 to Ala). This residue has previously been shown to be critical in maintaining the serum persistence of a murine IgG_1 Fc fragment in mice (*10*). The Glutamine Synthetase Gene Amplification System was used to produce the chTNT-3 mutant in mammalian cells, so that sufficient quantities of the recombinant antibody could be generated for preclinical studies and patient trials, if warranted. It was possible to use protein A affinity chromatography for purification of the chTNT-3 mutant, despite the previous report that this amino acid substitution in the murine γ_1 Fc fragment greatly impaired binding to Staphylococcal protein A (*10*), which was anticipated because of overlap with a protein A binding site (*27*). The retention of protein A binding makes purification of the chTNT-3 mutant as straightforward as that of the parental chimeric antibody, and obviates purification using alternative methods such as a histidine tag with a Ni^{2+} column.

As expected, the chTNT-3 mutant retained the high affinity of chTNT-3, as demonstrated by radioimmunoassay and Scatchard analysis. The pharmacokinetic behavior of chTNT-3, however, was significantly altered by the amino acid substitution. The mutant was eliminated extremely rapidly from BALB/c mice, compared to the relatively slow whole-body clearance of chTNT-3 (Fig. 1). This finding is in agreement with the results of Ward et al. (*10,11*), who examined the influence of this and other residues conserved among murine and human immunoglobulin isotypes on antibody catabolism, by generating Fc mutants derived from murine IgG_1. The current study extends their findings to the human IgG_1 isotype and to an intact IgG, which supports their contention that similar effects on clearance would be expected for human antibodies (*9*). For this reason, we anticipate that similarly dramatic differences in clearance will be observed in patients.

The impact of this amino acid substitution on the biodistribution of the chTNT-3 mutant in colon tumor-bearing mice was remarkable both in normal tissues and in tumor xenografts (Tables 1–3). Because chTNT-3 and the mutant are indistinguishable in other respects, these findings represent clear evidence that whole-body half-life is a critical determinant of the magnitude of tumor uptake. Similar differences in both clearance and tissue biodistribution have been reported previously for C_H2 domain-deleted chimeric antibodies (*28,29*). The impact of these deletions, however, resulted in a greater acceleration of β phase clearance than did the amino acid substitution described in this report. The domain-deleted ch14.18 MAb was shown to have a β $t_{1/2}$ of 12 h (*28*), and the domain-deleted cB72.3 had a half-life of 7.8 h (*29*). The faster clearance of these C_H2 domain-deleted chimeric antibodies compared to the chTNT-3 mutant may be attributable to the difference in molecular weights or, alternatively, to a greater impact on binding to the FcRn. The tumor uptake of the antibodies lacking the C_H2 domain was a small fraction of the uptake of the corresponding parental MAbs 24 or 72 h postinjection, compared to the relatively

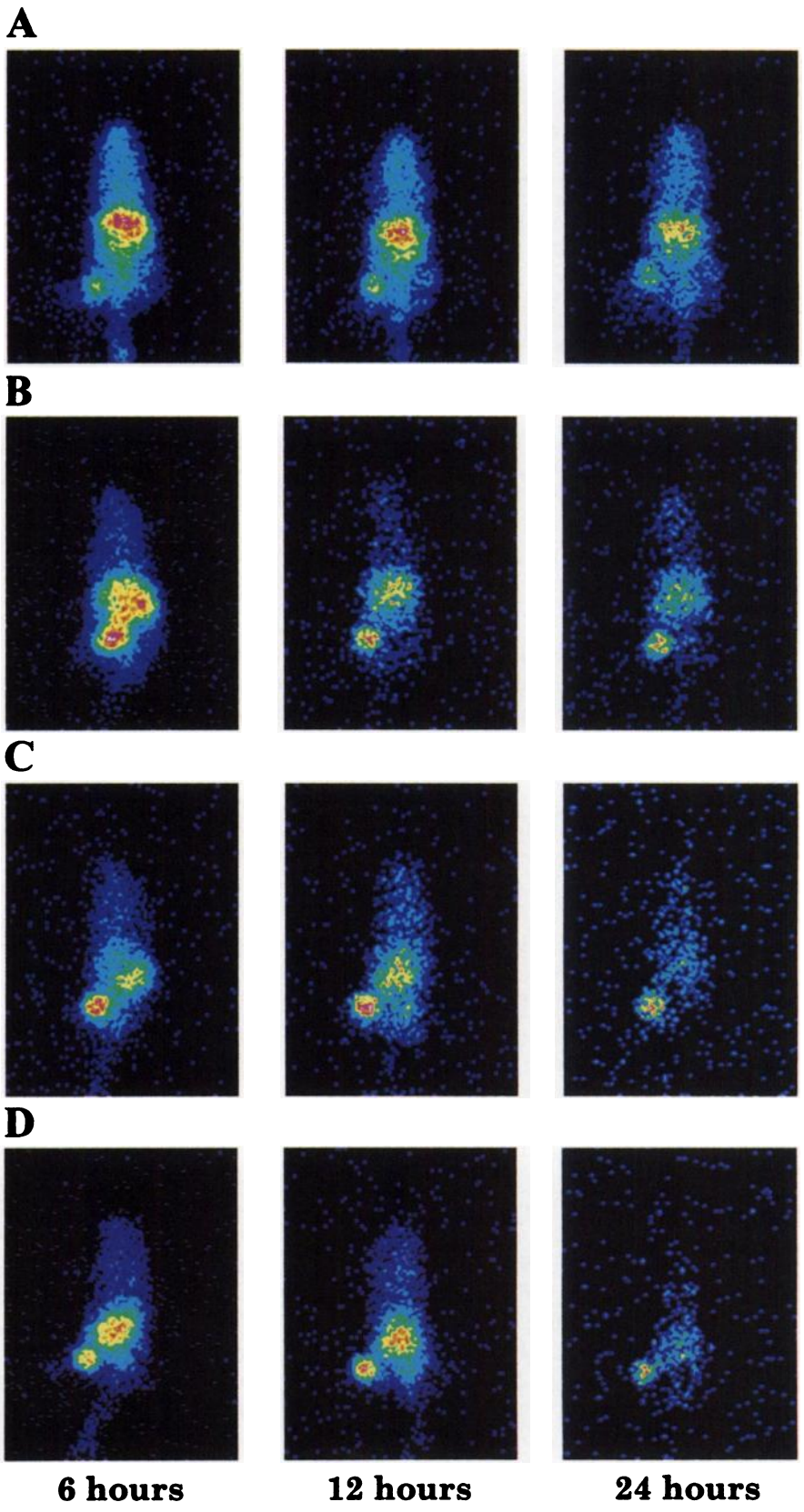

FIGURE 2. Images of tumor-bearing nude mice with chimeric antibodies at indicated times after injection, using Nuclear MAX Plus image analysis software package. (A) LNCaP human prostate tumor-bearing mice injected with ^{99m}Tc-labeled chTNT-3. (B) LNCaP human prostate tumor-bearing mice injected with ^{99m}Tc-labeled chTNT-3 mutant. (C) LS174T human colon tumor-bearing mice injected with ^{99m}Tc-labeled chTNT-3 mutant. (D) A427 human lung tumor-bearing mice injected with ^{99m}Tc-labeled chTNT-3 mutant.

TABLE 4
24-Hour Biodistribution of ^{99m}Tc-Labeled chTNT-3 Mutant in LS174T Human Colon Adenocarcinoma Tumor-Bearing Nude Mice

Organ	%ID/g
Blood	0.31 ± 0.05
Skin	0.34 ± 0.10
Muscle	0.09 ± 0.08
Bone	0.13 ± 0.05
Heart	0.10 ± 0.02
Lung	0.25 ± 0.06
Liver	0.64 ± 0.03
Spleen	0.28 ± 0.05
Pancreas	0.06 ± 0.01
Stomach	0.16 ± 0.02
Intestine	0.08 ± 0.00
Kidney	2.43 ± 0.13
Tumor	1.76 ± 0.12

Data are mean ± SD.

high tumor uptake observed with the chTNT-3 mutant (36% of chTNT-3 24 h postinjection). The fact that the chTNT-3 mutant retains the capacity to bind to protein A, in contrast to the C_H2 domain-deleted MAbs, lends this product to straightforward and inexpensive purification.

The chTNT-3 mutant exhibits pharmacokinetic behavior intermediate between that of intact MAbs and derived fragments. Thus, the decreased tumor accretion of the mutant is less than the decrease in tumor uptake observed for Fab′ fragments. Moreover, the lack of accumulation of signal in the kidneys with ^{125}I-labeled chTNT-3 mutant, in contrast to the predominant renal clearance of Fab′ fragments (*5,6*), should result in improved discrimination of abdominal tumors with radiolabeled chTNT-3 mutant. Direct comparisons between antibody fragments and intact MAbs with single amino acid substitutions must be made in clinical studies, however, to determine the appropriate clinical settings for the use of antibody mutants.

The immunoscintigraphic results presented in this report demonstrate the ability of the chTNT-3 mutant to target diverse solid tumors (Fig. 2). These data are consistent with previously published findings using chTNT-3 and a fusion protein containing chTNT-3 and interleukin-2 (*13,30*). Indeed, because of the specificity of chTNT-3 for a universal nuclear antigen exposed in degenerating and necrotic cells, it is anticipated that products derived from this MAb will have applications in targeting the majority of human solid tumors. Imaging with the chTNT-3 mutant may find utility not only in the diagnosis and staging of cancers, but also in the identification of patients for whom TNT radioimmunotherapy would have the most benefit. In addition, imaging with this product may be useful for monitoring the progress of various therapeutic modalities by imaging new areas of degeneration and necrosis resulting from cancer treatments. Determination of the magnitude of the acceleration in clearance in humans produced by this amino acid substitution in chTNT-3 awaits clinical evaluation. Such studies will also suggest the most appropriate diagnostic radionuclide for imaging with the chTNT-3 mutant, which will depend on the whole-body half-life of this product in patients.

CONCLUSION

The accelerated clearance produced by a single amino acid substitution in the Fc region of chTNT-3 leads to improved imaging in mice bearing diverse human tumor xenografts. These studies suggest that a rapidly clearing antibody mutant generated by this approach may be useful for the immunoscintigraphy of human tumors.

ACKNOWLEDGMENTS

This study was supported in part by Cancer Therapeutics, Inc. (Los Angeles, CA), Techniclone Corp. (Tustin, CA), and Brilliance Pharmaceuticals (Shanghai, China).

REFERENCES

1. Doerr RJ, Abdel-Nabi H, Krag D, Mitchell E. Radiolabeled antibody imaging in the management of colorectal cancer: results of a multicenter clinical study. *Ann Surg.* 1991;214:118–124.
2. Moffat FL, Pinsky CM, Hammershaimb L, et al. Clinical utility of external immunoscintigraphy with the IMMU-4 technetium-99m Fab′ antibody fragment in patients undergoing surgery for carcinoma of the colon and rectum: results of a pivotal, phase III trial. *J Clin Oncol.* 1996;14:2295–2305.
3. Breitz HB, Tyler A, Bjorn MJ, Lesley T, Weiden PL. Clinical experience with Tc-99m nofetumomab merpentan (Verluma) radioimmunoscintigraphy. *Clin Nucl Med.* 1997;22:615–620.
4. Kahn D, Williams RD, Haseman MK, Reed NL, Miller SJ, Gerstbrein J. Radioimmunoscintigraphy with In-111-labeled capromab pendetide predicts prostate cancer response to salvage radiotherapy after failed radical prostatectomy. *J Clin Oncol.* 1998;16:284–289.
5. Behr T, Becker W, Hannappel E, Goldenberg DM, Wolf F. Targeting of liver metastases of colorectal cancer with IgG, F(ab′)$_2$, and Fab′ anti-carcinoembryonic antigen antibodies labeled with ^{99m}Tc: the role of metabolism and kinetics. *Cancer Res.* 1995;55(suppl):5777S–5785S.
6. Podoloff DA, Patt YZ, Curley SA, Kim EE, Bhadkamkar VA, Smith RE. Imaging of colorectal carcinoma with technetium-99m radiolabeled Fab′ fragments. *Semin Nucl Med.* 1993;23:89–98.
7. Buist MR, Kenemans P, den Hollander W, et al. Kinetics and tissue distribution of the radiolabeled chimeric monoclonal antibody MOv18 IgG and F(ab′)$_2$ fragments in ovarian carcinoma patients. *Cancer Res.* 1993;53:5413–5418.
8. Behr TM, Becker WS, Bair H-J, et al. Comparison of complete versus fragmented technetium-99m-labeled anti-CEA monoclonal antibodies for immunoscintigraphy in colorectal cancer. *J Nucl Med.* 1995;36:430–441.
9. Ghetie V, Ward ES. FcRn: the MHC class I-related receptor that is more than an IgG transporter. *Immunol Today.* 1997;18:592–598.
10. Kim J-K, Tsen M-F, Ghetie V, Ward ES. Identifying amino acid residues that influence plasma clearance of murine IgG1 fragments by site-directed mutagenesis. *Eur J Immunol.* 1994;24:542–548.
11. Medesan C, Matesoi D, Radu C, Ghetie V, Ward ES. Delineation of the amino acid residues involved in transcytosis and catabolism of mouse IgG1. *J Immunol.* 1997;158:2211–2217.
12. Ghetie V, Popov S, Borvak J, et al. Increasing the serum persistence of an IgG fragment by random mutagenesis. *Nature Biotechnol.* 1997;15:637–640.
13. Hornick JL, Sharifi J, Khawli LA, et al. A chemically modified chimeric TNT-3 monoclonal antibody directed against DNA for the radioimmunotherapy of solid tumors. *Cancer Biother Radiophar.* 1998;13:255–268.
14. Pulvertaft RJV. Cytology of Burkitt's tumour (African lymphoma). *Lancet.* 1964;1:238–240.
15. Ohsugi Y, Gershwin ME, Owens RB, Nelson-Rees WA. Tumorigenicity of human malignant lymphoblasts: comparative study with unmanipulated nude mice, antilymphocyte serum-treated nude mice, and X-irradiated nude mice. *J Natl Cancer Inst.* 1980;65:715–718.

16. Tom BH, Rutzky LP, Jakstys MM, Oyasu R, Kaye CI, Kahan BD. Human colonic adenocarcinoma cells. I. Establishment and description of a new line. *In Vitro.* 1976;12:180–191.
17. Giard DJ, Aaronson SA, Todaro GJ, et al. In vitro cultivation of human tumors: establishment of cell lines derived from a series of solid tumors. *J Natl Cancer Inst.* 1973;51:1417–1423.
18. Horoszewicz JS, Leong SS, Kawinski E, et al. LNCaP model of human prostatic carcinoma. *Cancer Res.* 1983;43:1809–1818.
19. Hu P, Glasky MS, Yun A, et al. A human-mouse chimeric Lym-1 monoclonal antibody with specificity for human lymphomas expressed in a baculovirus system. *Hum Antibodies Hybridomas.* 1995;6:57–67.
20. Laemmli UK. Cleavage of structural proteins during the assembly of the head of bacteriophage T4. *Nature.* 1970;227:680–685.
21. Alauddin MM, Khawli LA, Epstein AL. An improved method of direct labeling monoclonal antibodies with technetium-99m. *Nucl Med Biol.* 1992;19:445–454.
22. Frankel ME, Gerhard W. The rapid determination of binding constants for antiviral antibodies by a radioimmunoassay: an analysis of the interaction between hybridoma proteins and influenza virus. *Mol Immunol.* 1979;16:101–106.
23. Epstein AL, Marder RJ, Winter JN, Fox RI. Two new monoclonal antibodies (LN-1, LN-2) reactive in B5 formalin-fixed, paraffin-embedded tissues with follicular center and mantle zone human B lymphocytes and derived tumors. *J Immunol.* 1984;133:1028–1036.
24. Zuckier LS, Georgescu L, Chang CJ, Scharff MD, Morrison SL. The use of severe combined immunodeficiency mice to study the metabolism of human immunoglobulin G. *Cancer.* 1994;73:794–799.
25. Hornick JL, Khawli LA, Hu P, Lynch M, Anderson PM, Epstein AL. Chimeric CLL-1 antibody fusion proteins containing granulocyte-macrophage colony-stimulating factor or interleukin-2 with specificity for B-cell malignancies exhibit enhanced effector functions while retaining tumor targeting properties. *Blood.* 1997;89:4437–4447.
26. John E, Thakur ML, Wilder S, Alauddin MM, Epstein AL. Technetium-99m-labeled monoclonal antibodies: influence of technetium-99m binding sites. *J Nucl Med.* 1994;35:876–881.
27. Deisenhofer J. Crystallographic refinement and atomic models of a human Fc fragment and its complex with fragment B of protein A from *Staphylococcus aureus* at 2.9- and 2.8-Å resolution. *Biochemistry.* 1981;20:2361–2370.
28. Mueller BM, Reisfeld RA, Gillies SD. Serum half-life and tumor localization of a chimeric antibody deleted of the C_H2 domain and directed against the disialoganglioside GD2. *Proc Natl Acad Sci USA.* 1990;87:5702–5705.
29. Slavin-Chiorini DC, Horan Hand P, Kashmiri SVS, Calvo B, Zaremba S, Schlom J. Biologic properties of a C_H2 domain-deleted recombinant immunoglobulin. *Int J Cancer.* 1993;53:97–103.
30. Hornick JL, Khawli LA, Hu P, Sharifi J, Khanna C, Epstein AL. Pretreatment with a monoclonal antibody/interleukin 2 fusion protein directed against DNA enhances the delivery of therapeutic molecules to solid tumors. *Clin Cancer Res.* 1999;5:51–60.